Interaction Between Permeation and Gating in a Putative Pore Domain Mutant in the Cystic Fibrosis Transmembrane Conductance Regulator

Zhi-Ren Zhang,* Stefan I. McDonough,† and Nael A. McCarty*

*Departments of Physiology and Pediatrics, Center for Cell and Molecular Signaling, Emory University School of Medicine, Atlanta, Georgia 30322, and †Division of Biology, California Institute of Technology, Pasadena, California 91125 USA

ABSTRACT The cystic fibrosis transmembrane conductance regulator (CFTR) is a chloride channel with distinctive kinetics. At the whole-cell level, CFTR currents in response to voltage steps are time independent for wild type and for the many mutants reported so far. Single channels open for periods lasting up to tens of seconds; the openings are interrupted by brief closures at hyperpolarized, but not depolarized, potentials. Here we report a serine-to-phenylalanine mutation (S1118F) in the 11th transmembrane domain that confers voltage-dependent, single-exponential current relaxations and moderate inward rectification of the macroscopic currents upon expression in *Xenopus* oocytes. At steady state, the S1118F-CFTR single-channel conductance rectifies, corresponding to the whole-cell rectification. In addition, the open-channel burst duration is decreased 10-fold compared with wild-type channels. S1118F-CFTR currents are blocked in a voltage-dependent manner by diphenylamine-2-carboxylate (DPC); the affinity of S1118F-CFTR for DPC is similar to that of the wild-type channel, but blockade exhibits moderately reduced voltage dependence. Selectivity of the channel to a range of anions is also affected by this mutation. Furthermore, the permeation properties change during the relaxations, which suggests that there is an interaction between gating and permeation in this mutant. The existence of a mutation that confers voltage dependence upon CFTR currents and that changes kinetics and permeation properties of the channel suggests a functional role for the 11th transmembrane domain in the pore in the wild-type channel.

INTRODUCTION

The cystic fibrosis transmembrane conductance regulator (CFTR) is an epithelial Cl^- channel activated by protein kinase A phosphorylation plus ATP hydrolysis (Gadsby and Nairn, 1997). A member of the ABC transporter superfamily (Higgins, 1992), the CFTR molecule is made up of two nonidentical halves, each consisting of six transmembrane-spanning (TM) domains followed by a consensus nucleotide binding domain (NBD). The two modules are joined by a regulatory (R) domain that is unique among ABC transporters (Riordan et al., 1989). CFTR has been heterologously expressed both transiently and permanently in many cell types, including *Xenopus* oocytes (Drumm et al., 1990; Bear et al., 1991), insect SF-9 cells (Kartner et al., 1991), and mammalian cultured cell lines (e.g., Rich et al., 1990); purified CFTR protein has also been studied in bilayer reconstitution experiments (Bear et al., 1992). In all of these systems, CFTR currents display similar kinetics. At the whole-cell level, CFTR currents are time independent. At the single-channel level, the conductance does not change with time after a step to a new voltage, and the channels display prolonged openings, for up to tens of seconds at a time. The single channels are uninterrupted at depolarizing potentials but interrupted at hyperpolarizing potentials by brief, flickery closings (McCarty et al., 1993; Fischer and Machen, 1994).

Structure-function studies using a variety of techniques are currently being applied to determine what portions of the protein make up the channel pore (Sheppard and Welsh, 1999). At this point, investigators have shown that residues in transmembrane domain 1 (TM1), TM2, TM3, TM5, and TM6 in the N-terminal half of the protein contribute to the pore. In the C-terminal half, only TM12 has been shown to contribute (McDonough et al., 1994). It was recently shown that channels can be formed from the C-terminal half of the CFTR molecule, with or without the R-domain, but that these channels exhibited reduced conductance in Cl^- and poor ability to select between halide anions (Devidas et al., 1998). It is also a distinct possibility that two full-length molecules are required to dimerize to form the functional channel (Zerhusen et al., 1998). Despite this body of work, the complete structure of the channel and the role of pore-lining domains in the function of the wild-type (WT) channel remain unknown.

Here we report a serine-to-phenylalanine mutation (S1118F) in TM11 that affects both permeation and gating. Most strikingly, the macroscopic S1118F-CFTR currents display voltage-dependent current relaxations; these relaxations are modulated by permeating anions. At steady state, the macroscopic (I/V) and single-channel (i/V) current-voltage relations also rectify inwardly. These results have implications for our understanding of how phosphorylation and ATP hydrolysis are coupled with the opening of the channel and imply a functional role for the 11th transmembrane domain in pore formation. Furthermore, they suggest

Received 21 July 1999 and in final form 28 March 2000.

Address reprint requests to Dr. Nael A. McCarty, Department of Physiology, Emory University School of Medicine, 1648 Pierce Drive, Atlanta, GA 30322-3110. Tel.: 404-727-1372; Fax: 404-727-2648; E-mail: NMCC@physio.emory.edu.

Dr. McDonough's present address is Marine Biological Laboratory, Woods Hole, MA 02543.

0006-3495/00/07/298/16 $2.00

that the pore of CFTR is not static, but rather may undergo conformational changes linked to gating of the channel. Portions of these data have been published in preliminary form (McDonough et al., 1998; McCarty and Zhang, 1998a; McDonough, 1994).

MATERIALS AND METHODS

Most methods were described in detail previously (McCarty et al., 1993; McDonough et al., 1994).

Preparation of oocytes and cRNA

CFTR was subcloned into the pALTER vector (Promega), and the S1118F, S1118A, and S1118F/F1111S mutations were made using the Promega Altered Sites protocol (McDonough et al., 1994). Capped transcripts (5–38 ng) were coinjected with 0.6 ng of β_2-adrenergic receptor cRNA into stage V *Xenopus* oocytes (McCarty et al., 1993). Oocytes were incubated in modified Liebovitz's L-15 medium with the addition of *N*-(2-hydroxyethyl)piperazine-*N*′-(2-ethanesulfonic acid) (HEPES) (pH 7.5), gentamicin, and penicillin/streptomycin. Recordings were made 24–72 h after the injection of transcripts.

Electrophysiology

Two-electrode voltage-clamp data were acquired at room temperature (~22°C) with a GeneClamp 500 amplifier and pCLAMP software (Axon Instruments, Foster City, CA). Normal bath solution for whole-cell experiments (ND96) contained (in mM) 96 NaCl, 2 KCl, 1 $MgCl_2$, and 5 HEPES (pH 7.5). The corner frequency was 500 Hz. When a Ag/AgCl pellet was used for the ground, the clamp settled in <2 ms. Time constants for the voltage-jump relaxations were determined by a least-squares fit to a single exponential; data for relaxations were fit from ~3 ms after the voltage jump to the steady-state portion of the curve.

For selectivity experiments, NaCl was replaced with the Na^+ salt of each of the anions studied. An agar bridge (3 M KCl in 3% agar) served as the ground. Data are corrected for junction potentials at the ground bridge, which ranged from 0.2 to 2.4 mV, as determined with a free-flowing KCl electrode. CFTR channels in oocytes were activated with isoproterenol in ND96 and alternately assayed in the presence of a Cl^--containing bath or a substitute anion. Substitutions were always made in the same order and for a 1-min duration: acetate, bromide, gluconate, glutamate, iodide, nitrate, isethionate, perchlorate, and thiocyanate. Brief exposure to substitute anions would not be expected to alter cytoplasmic chloride concentration to a significant degree. To control for changes in the level of activation, data for each substitute anion were bracketed with data in Cl^- plus isoproterenol before and after the substitute anion (e.g., Cl^- + isoproterenol; acetate; Cl^- + isoproterenol; Br^-; etc.). Control experiments (not shown) indicated that selectivity for WT was not altered by isoproterenol.

For several experiments, macroscopic currents were assayed over two separate time periods during a voltage step protocol. In experiments testing the time-dependent shift in the current-voltage relation in Cl^--containing solutions, we defined "instantaneous" currents as the averaged currents at each potential during the first 5 ms after the capacitative transient. "Steady-state" currents are the averaged currents at each potential during the last 5 ms of the voltage step. For experiments investigating selectivity, the "early" and "late" periods correspond, respectively, to the first and last 10 ms of the 75-ms voltage step protocol.

Single-channel recordings were performed at room temperature (~22°C) with either a GeneClamp 500 or an AI2120 amplifier (Axon). Oocytes were prepared for study by shrinking in hypertonic solution (in mM: 200 monopotassium aspartate, 20 KCl, 1 $MgCl_2$, 10 EGTA, and 10 HEPES-KOH, pH 7.2), followed by manual removal of the vitelline membrane. Pipettes were pulled in four stages from borosilicate glass (Sutter) and had resistances averaging ~10 MΩ when filled with pipette solution. For single-channel experiments on excised inside-out patches, the pipette solution contained (in mM) 150 *N*-methyl-D-glucamine-Cl^-, 5 $MgCl_2$, and 10 N-tris-(hydroxymethyl) methyl-2-aminoethanesulfonic acid (TES), adjusted to pH 7.4 with Tris. Intracellular (cytoplasmic) solution contained (in mM) 150 NMDG-Cl^-, 1.1 $MgCl_2$, 2 Tris-EGTA, 1 MgATP, and 10 TES, adjusted to pH 7.4 with Tris. CFTR channels were activated before patch excision by the addition of 1–5 μM isoproterenol to the bath solution. PKA (50 U/ml; Promega) was added to the intracellular solution to maintain phosphorylation. Patch currents were recorded at 10 kHz on DAT tape (Sony model DTC-790). For subsequent analysis, records were filtered at 1 kHz or 100 Hz and acquired by the computer at 4 kHz or 400 Hz, using the pCLAMP software (Axon).

Digitized records were analyzed using Igor Pro, version 3.11 (Wavemetrics, Lake Oswego, OR). For open-time analysis to assay burst duration, open bursts were defined as intervals separated by closings of 80 ms or greater, a value previously established to discriminate between ATP-dependent gating and intraburst blockade of CFTR in mammalian cells (Zeltwanger et al., 1999) and in oocytes (Zhang et al., 2000). All recordings used in this analysis contained only one active channel, as judged by the lack of simultaneous open levels.

Source of reagents

Unless otherwise noted, all reagents were obtained from Sigma Chemical Co. (St. Louis, MO). Diphenylamine-2-carboxylate (DPC) was from Aldrich Chemical Co. (Milwaukee, WI); L-15 media was from Gibco/BRL (Gaithersburg, MD). Sodium salts of the following anions were from Fisher Scientific (Fair Lawn, NJ): chloride, nitrate, iodide, perchlorate, and acetate. Sodium bromide and sodium thiocyanate were from J. T. Baker Scientific (Phillipsburg, NJ).

Statistics

Unless otherwise noted, values given are means ± SE. Statistical analysis was performed using the *t*-test for unpaired measurements by SigmaStat (Jandel Scientific, San Rafael, CA), with $p \leq 0.05$ or $p \leq 0.01$ considered indicative of significance. For comparisons of selectivity experiments, where instantaneous data were compared to steady-state data in the same oocytes, the paired *t*-test was used. Most figures include error bars; these are only visible when they exceed the size of the symbols.

RESULTS

Steady-state macroscopic *I/V* relations and voltage-jump relaxations

Based upon our proposed alignment and conservation of positioning of polar residues (Fig. 1 *A*), we model TM11 as potentially contributing to the pore of the CFTR channel. In constructing this alignment, which merely serves as a working model, we began with the alignment of TM6 and TM12, which was proposed previously (McDonough et al., 1994). To extend this to TM5 and TM11, these sequences were represented in inverted orientation, such that the four TMs would have their extracellular ends and intracellular ends in common, as they would be in the folded peptide. Subsequently, the alignment was optimized by shifting the sequences of TM5 and TM11 such that the bands of hydroxy-

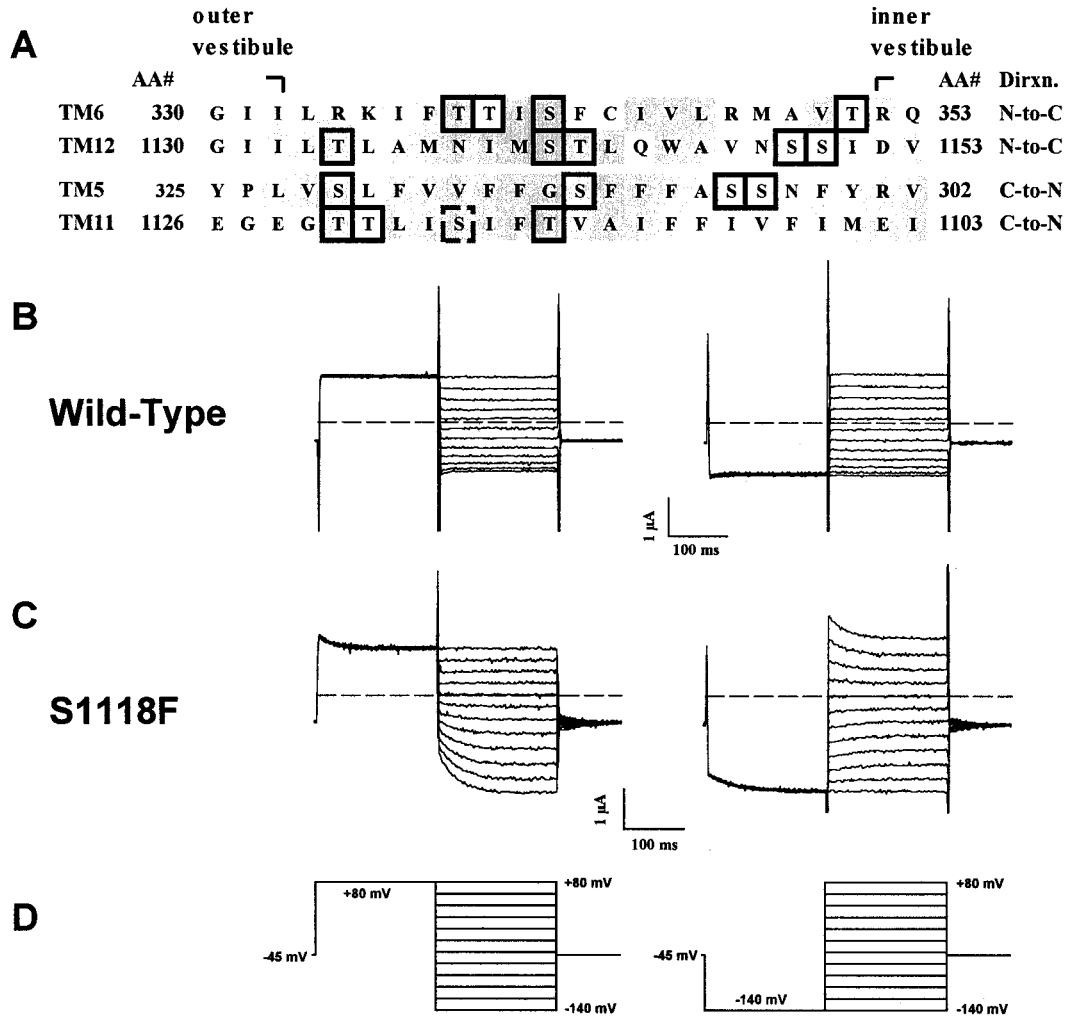

FIGURE 1 Mutation S1118F-CFTR results in current relaxations. (*A*) Proposed alignment of putative pore-forming TM helices. Note that TM5 and TM11 are inverted with respect to TM6 and TM12, such that the extracellular ends and intracellular ends are oriented appropriately. Hydroxylated residues, which we believe make important contributions to permeation, are boxed. S1118 is the sole serine in TM11. Shaded positions indicate similarity of amino acid character (i.e., hydrophobic, polar, etc.). (*B* and *C*) Families of currents measured in oocytes expressing either wild-type or S1118F-CFTR channels, respectively. Currents were evoked using the voltage-clamp protocol shown in *D*. *Left traces*: Depolarizing prepotential. *Right traces*: Hyperpolarizing prepotential. The dashed line in *B* and *C* represents the zero-current level. Note that relaxations reversed around E_{Cl} in the mutant.

lated residues in TM5 and TM11 were placed in positions equivalent to those of the hydroxylated residues that are prominent in the extracellular halves of TM6 and TM12.

According to this alignment, S1118 occupies a position that would be predicted to face into the pore. Hence we were initially interested in determining whether the nature of the amino acid at this position contributes to the permeation properties of CFTR. Unexpectedly, the most obvious consequence of the mutation of S1118F-CFTR is the appearance of relaxations in current density upon stepping to a new membrane potential. Fig. 1 *B* shows wild-type currents in response to two different voltage pulse protocols (shown in Fig. 1 *D*). In the traces shown on the left, the membrane potential was stepped from −140 mV to +80 mV for 200 ms in increments of +20 mV after a 200-ms prepulse to +80 mV (depolarizing prepotential). The traces shown at right indicate currents responding to the same step protocol (−140 to +80 mV), but after a 200-ms prepulse to −140 mV (hyperpolarizing prepotential). WT-CFTR currents show time-independent behavior with both protocols. However, S1118F-CFTR displays voltage-dependent current relaxations in response to protocols applying either depolarizing or hyperpolarizing prepotentials. After a jump to a new membrane potential, the current jumps instantaneously then relaxes over a time course of a few tens of milliseconds to a new steady-state level. These voltage-jump relaxations lead to a larger conductance for jumps to more negative potentials and to a smaller conductance for jumps in the

opposite direction. Both relaxations were fit by a single exponential time course, shown superimposed over the expanded traces in Fig. 2. This time constant measured ~26 ms for the steps to −140, −120, −100, and −80 mV with a depolarizing prepotential; with a hyperpolarizing prepotential, the time constants for the relaxations at +40, +60, and +80 mV displayed moderate voltage dependence and measured 22.6 ± 1.0 ms at +80 mV (Fig. 2 *C*). This voltage dependence may arise from sensitivity to the direction of ion flow. The relaxations were largely unaffected by replacement of the 1 mM $MgCl_2$ in the bath solution with 1 mM $CaCl_2$ (Fig. 2 *C*). This implies that the relaxations are due to channel gating, rather than to introduction of a binding site for Mg^{2+} to block the channel, although we cannot rule out the possibility that both Ca^{2+} and Mg^{2+} block and do so with equal affinity. Note that S1118F-CFTR also displays tail currents (Figs. 1, 2, 6, and 7), which have not been described for WT or any mutant of CFTR studied thus far.

Fig. 3 shows that the macroscopic current-voltage relations shift during the course of the relaxations. In both of the *I*/*V* relations shown, instantaneous current was calculated as the mean current over the first 5 ms of each trace after the prepulse; steady-state current is the mean of the last 5 ms at each potential. After a depolarizing prepulse (protocol of Fig. 1 *D*, *left*), the instantaneous currents exhibit a nearly linear *I*/*V* relation, reversing at ~0 mV (Fig. 3 *A*). At steady state, outward currents are identical to instantaneous currents. However, the steady-state *I*/*V* relation shifts around an inflection point at the reversal potential, such that inward currents at steady state are greater than instantaneous currents at the same potentials. This leads to an inwardly rectifying steady-state *I*/*V*. The shift in *I*/*V* relations for experiments that utilized a hyperpolarizing prepulse are more complex (Fig. 3 *B*), indicating that the processes underlying relaxations at the two voltage extremes may not be symmetrical. The instantaneous currents exhibit mild outward rectification, reversing at ~0 mV. Steady-state outward currents are reduced compared with instantaneous currents at the same potentials. This is consistent with the inverse of the results with a depolarizing prepulse. However, steady-state inward currents also diverge from the instantaneous currents, albeit to a lesser degree than do outward currents.

In WT-CFTR, TM11 contains four phenylalanine residues (Fig. 1 *A*); mutation of S1118F adds a fifth. If this domain is α-helical, as predicted from hydropathy analysis (Riordan et al., 1989), mutation S1118F would then place three phenylalanine residues in close mutual proximity (at positions 1107, 1111, and 1118) and on approximately the same face of the helix. To determine whether this imposed pattern was the source of relaxations in S1118F-CFTR, due to introduction of another bulky residue, the double mutation S1118F/F1111S was constructed. These channels displayed relaxations indistinguishable from those of the single

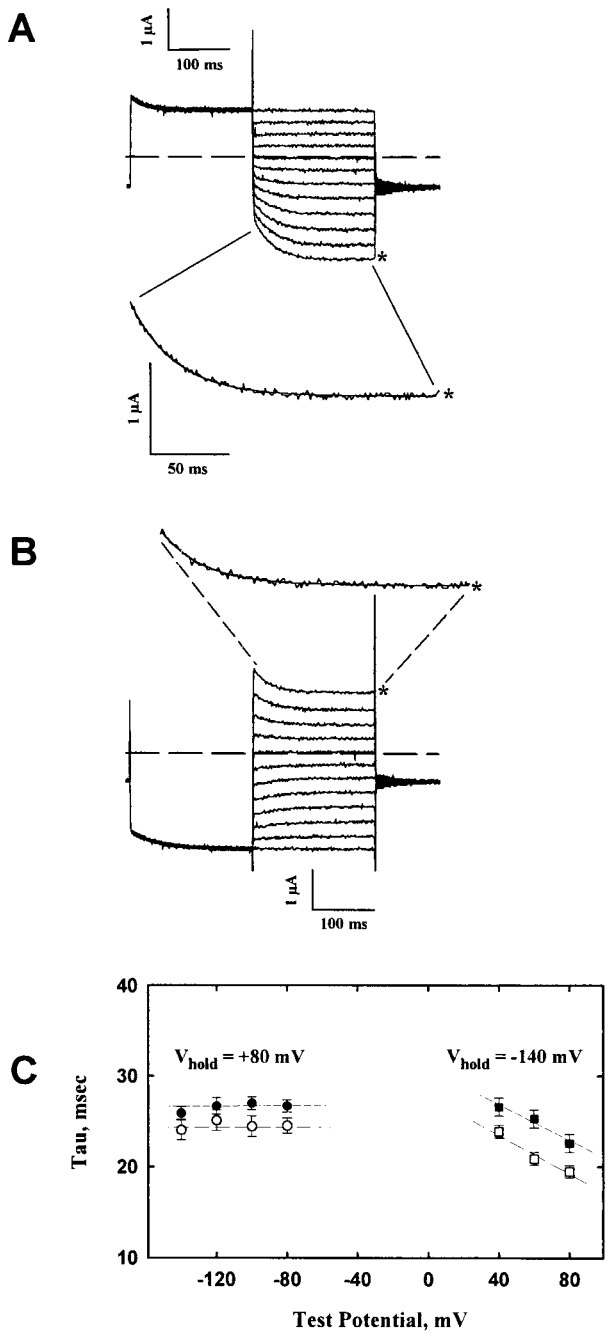

FIGURE 2 Relaxations induced in S1118F-CFTR currents were fit to single-exponential decay functions. (*A*) Traces for jumps after a depolarizing prepulse; the trace for −140 mV is in an expanded scale with a superimposed fit. (*B*) Traces for jumps after a hyperpolarizing prepulse; the trace for +80 mV is in an expanded scale with fit. (*C*) Time constants for hyperpolarizing test potentials (*left*) or depolarizing test potentials (*right*), after the appropriate prepulse, are shown as a function of test potential. ●, ■, Experiments with 1 mM Mg^{2+} in the bath; ○, □, experiments with 1 mM Ca^{2+}. Points represent the mean ± SE for $n = 7$ (Mg^{2+}) or 5 (Ca^{2+}) oocytes. These relaxations are not seen in S1118A channels (not shown).

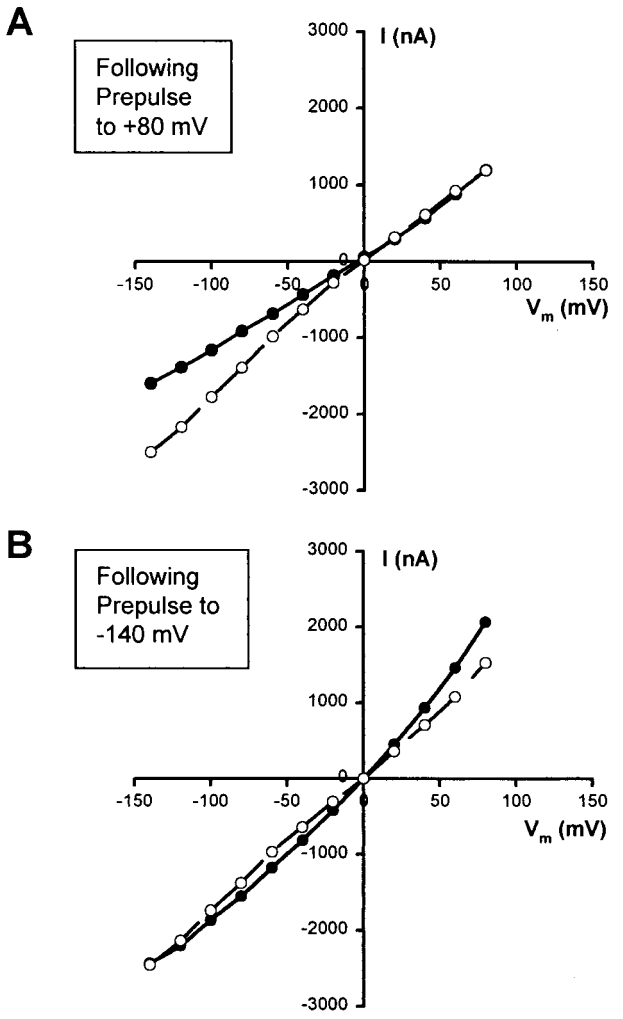

FIGURE 3 The current-voltage relations for S1118F-CFTR channel shift during the voltage-jump relaxations. Instantaneous currents (●) were measured as the average currents over the first 5 ms after the capacitative transient. Steady-state currents (○) are the average currents over the final 5 ms at each potential. (*A*) Currents observed at several test potentials after a depolarizing prepulse (Fig. 1 *D*, *left*) show the development of pronounced inward rectification. Only inward currents shift during the relaxation. For current traces after a depolarizing prepulse, the ratio of instantaneous to steady-state current (I_{inst}/I_{SS}) at −140 mV was 0.64 ± 0.01 (n = 6). (*B*) Currents observed after a hyperpolarizing prepulse (Fig. 1 *D*, *right*) show the development of a complex rectification pattern affecting both inward and outward currents. For current traces after a hyperpolarizing prepulse, (I_{inst}/I_{SS}) at +80 mV was 1.35 ± 0.01. Data shown are for one representative oocyte.

mutant S1118F-CFTR (not shown). Although certainly not definitive, this supports the hypothesis that the relaxations are due to a specific effect at position 1118 (however, there is no reason to believe, a priori, that residues at the extracellular end of TM11 make a contribution to the pore equivalent to that made by residues at the cytoplasmic end). In addition, mutation of S1118 to alanine (S1118A-CFTR) did not cause relaxations. This implies that the presence of phenylalanine at position 1118, rather than the absence of the serine, may cause the relaxations.

Steady-state conductance and gating behavior in single channels

The whole-cell data indicate that the process underlying the relaxations begins immediately as the membrane potential is stepped to a new level and is essentially complete within 200 ms (Fig. 1 *C*). One potential explanation for the introduction of voltage-jump relaxations is an effect on steady-state kinetics of CFTR channels. Gating behavior of single CFTR channels from oocytes expressing WT or S1118F-CFTR was studied in excised patch mode. Visual inspection of patch currents (Fig. 4) indicates that the open-state lifetimes of mutant channels are much briefer than those for WT channels measured under similar conditions, suggesting that the open state in the mutant was less stable than that in the WT channel. In no case did we observe patches with long-lasting open-channel bursts, as are commonly observed in WT channels in the presence of ATP. The open state was less stable at −100 mV membrane potential than at +100 mV (Fig. 5), as has been shown for WT (McCarty et al., 1993; Fischer and Machen, 1994). This state most likely represents block by TES in the intracellular solution, rather than actual gating closures (Zhang et al., 2000). We analyzed single-channel burst duration from records obtained in the presence of 1 mM ATP plus 50 U/ml PKA for mutant and WT channels. For this analysis, records were filtered at 100 Hz, which effectively ignores the brief flickery closed events introduced by the pH buffer; therefore, burst duration is equivalent to channel open time. Under these conditions, burst duration was 1392 ± 77 ms for WT-CFTR (n = 441 bursts) and 102 ± 8 ms for S1118F-

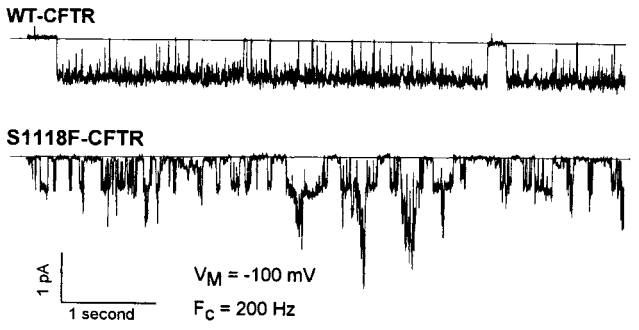

FIGURE 4 The mutation affects steady-state conductance and gating behavior. Single-channel records are from excised inside-out patches in the presence of 1 mM MgATP in the bath, clamped at V_m = −100 mV, and filtered at 200 Hz. Currents were acquired by the computer at 1 kHz. Horizontal lines indicate the closed level in each trace. Note that S1118F-CFTR channels exhibit much briefer openings than does WT. Currents were not observed in phosphorylated WT or S1118F-CFTR channels bathed in solutions lacking ATP (not shown).

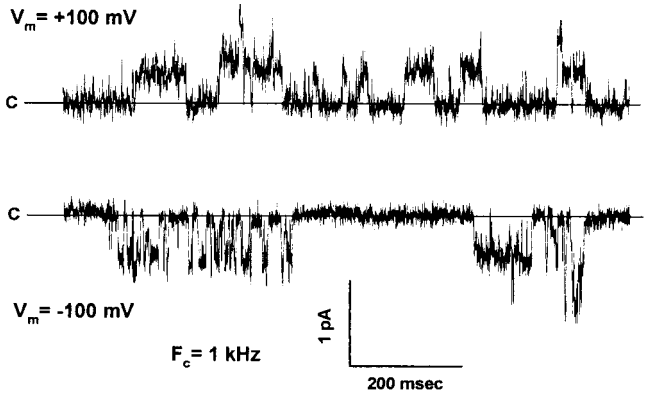

FIGURE 5 S1118F-CFTR channels show rectification of single-channel conductance. An excised patch recording at ±100 mV was made in the presence of 1 mM MgATP plus 50 U/ml PKA. The record was filtered at 1 kHz and acquired at 4 kHz. Note that conductance is smaller at depolarizing potentials than at hyperpolarizing potentials, despite the use of symmetrical 150 mM Cl^- solutions.

CFTR ($n = 391$ bursts). Hence the mean burst duration in S1118F-CFTR is reduced to only 7% that of WT channels.

The mutation also results in rectification of the single-channel conductance. All-points histograms were constructed from records filtered at 1 kHz. In symmetrical 150 mM chloride-containing solutions, the steady-state conductance was 5.1 ± 0.2 pS ($n = 5$) at +100 mV and 7.4 ± 0.2 pS ($n = 7$) at −100 mV. Hence the steady-state conductance rectifies in the direction expected from the decay in whole-cell experiments. In contrast, WT-CFTR single channels under identical conditions exhibit a linear i/V relation, with conductance averaging 8 pS (McCarty et al., 1993; McDonough et al., 1994; Zhang et al., 2000).

Because the data in Fig. 5 were collected long after the membrane potential was stepped to the voltages shown, the kinetic process(es) underlying the whole-cell current relaxations was essentially complete. It will be important to compare the voltage dependence of single-channel kinetics and conductance at steady state with those measured immediately after the voltage pulse. These experiments will be reported elsewhere.

The mutation has mild effects on block by a pore-blocking drug

DPC blocks CFTR by binding within the pore in a voltage-dependent manner (McCarty et al., 1993). The affinity and/or voltage dependence of this interaction are sensitive to mutations in some pore-lining residues and are sensitive to bath pH (McDonough et al., 1994; Zhang et al., 2000). We tested whether S1118F-CFTR exhibited alterations in the interaction with DPC, which would be consistent with a pore-lining position for this serine. Fig. 6 shows background-subtracted S1118F-CFTR currents for a representative cell before (Fig. 6 *A*) and several minutes after (Fig. 6 *B*) bath application of 200 μM DPC. DPC blocked inward currents at this concentration, as has been found previously for WT (McCarty et al., 1993). Current-voltage relations were constructed from the steady-state currents in the presence and absence of DPC (Fig. 6 *C*). Note that the unblocked currents (*open symbols*) show moderate inward rectification, compared to the stronger outward rectification seen for the wild-type channel; rectification of macroscopic currents was consistent with the rectification of single-channel currents. At −100 mV, DPC blocks S1118F-CFTR and WT channels with roughly the same efficacy: the apparent K_D (at −100 mV) was, respectively, 266 ± 13 μM and 276 ± 14 μM (mean ± SE, $n = 6$ and 15; data for WT are from McDonough et al., 1994). Woodhull (1973) analysis was used to calculate the apparent voltage dependence of block. Averaged values for K_D as a function of membrane voltage are plotted in Fig. 6 *D* and compared to block of the wild-type channel measured with the same protocol (*dotted line*). The voltage dependence of the S1118F-CFTR block is significantly less steep than that of the wild type; the apparent binding distance is $\theta = 0.27 \pm 0.01$ (mean ± SE, $n = 6$) for the mutant versus 0.41 ± 0.03 for WT channels (McDonough et al., 1994).

S1118F-CFTR exhibits altered permeation characteristics

S1118, according to our alignment, occupies a position in TM11 that is homologous to that of T338 in TM6. Hanrahan and co-workers (Linsdell et al., 1997b; Linsdell et al., 1998) have shown that mutation of T338 and the adjacent T339 led to changes in the selectivity pattern of CFTR channels expressed in Chinese hamster ovary cells. Our previous work indicates that hydroxylated residues (S, T) play important roles both in establishing sites for Cl^- conduction and in establishing the selectivity pattern of CFTR (McDonough et al., 1994; McCarty and Zhang, 1998b, 1999). Hence we attempted to determine whether mutations at S1118 resulted in altered selectivity characteristics.

Because oocytes expressing S1118F-CFTR show voltage-jump relaxations, it was not appropriate to use the more common approach of applying voltage-ramp protocols to generate selectivity data. Instead, currents in oocytes expressing WT-, S1118F-, or S1118A-CFTR channels were elicited by stepping for 75 ms from the holding potential of −30 mV to a series of test potentials between −140 and +80 mV in +20 mV increments. This voltage protocol elicited significant voltage-jump relaxations at depolarizing potentials, where currents arise from chloride entry, while relaxations at hyperpolarizing potentials were not as dramatic and were variable between oocytes (Fig. 7). If there are two open states that vary in the voltage dependence of microscopic kinetics, currents measured early in the relaxation and at later times likely represent different mixtures of

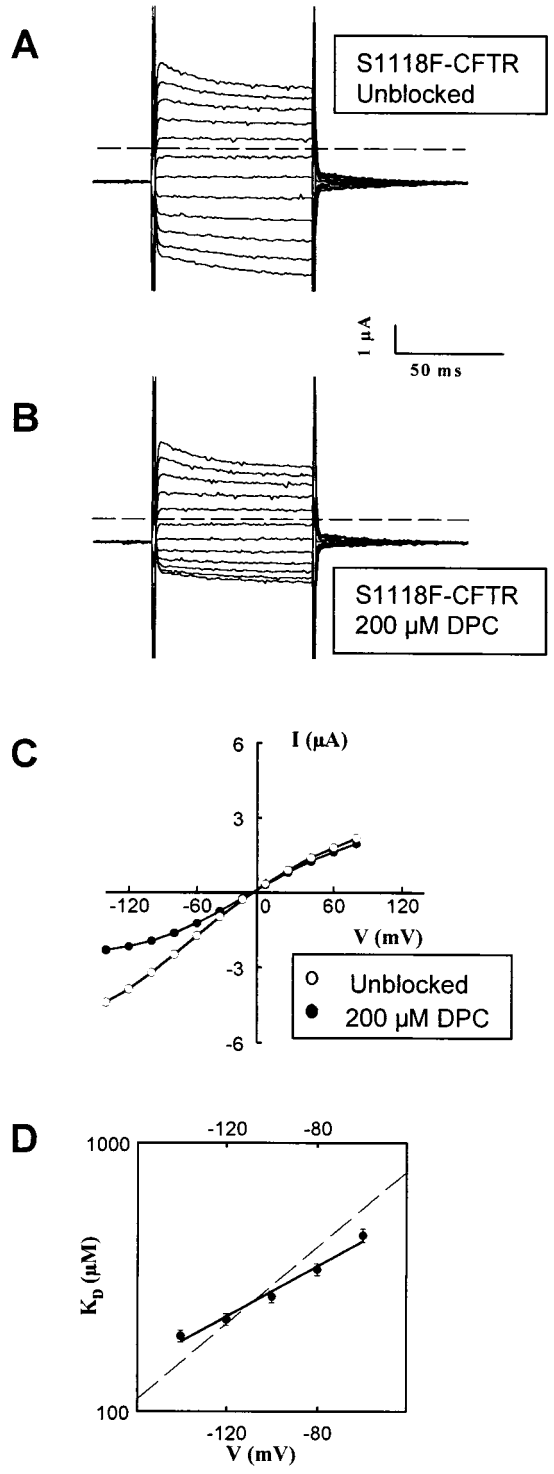

FIGURE 6 Mutation S1118F has mild effects on blockade by DPC. (*A* and *B*) Background-subtracted currents elicited by stepping for 75 ms from the holding potential of −45 mV to test potentials between −140 and +80 mV in +20-mV increments. The zero-current level is indicated by the dashed lines. (*A*) Unblocked currents. (*B*) Currents from the same cell incubated for ~7 min with 200 μM DPC. (*C*) Current-voltage relation for steady-state currents in the same cell. ○, unblocked currents; ●, currents with DPC. (*D*) Woodhull analysis of blockade. Each point is the mean ± SE for $n = 6$ oocytes. The straight line fit corresponds to a binding distance of $\theta = 0.27$. The dotted line represents the K_D versus voltage relation for WT-CFTR (McDonough et al., 1994), with $\theta = 0.41$.

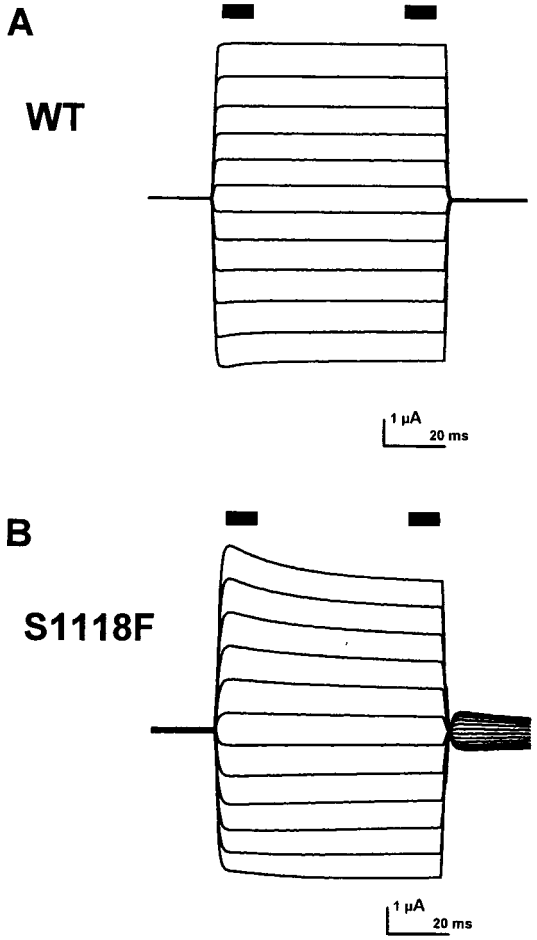

FIGURE 7 Current profiles for selectivity experiments. The membrane potential was held at −30 mV and stepped for 75 ms to test potentials between −140 and +80 mV in +20-mV increments. (*A*) WT currents, which show no time dependence of outward currents. Inward currents at the most hyperpolarizing potentials decay slightly because of low intracellular Cl^- and block by large cytoplasmic anions. (*B*) Currents in S1118F-CFTR-expressing oocytes, showing pronounced relaxations at depolarizing test potentials. Bars in *A* and *B* indicate the "early" and "late" time periods (10 ms each) used for analysis. S1118A-CFTR channels did not indicate time dependence with this protocol (not shown). Note the prominent tail currents in S1118F-CFTR but not in WT.

those two states, and these may differ in their permeation properties. With this voltage protocol, relaxations at test potentials more negative than +80 mV may not have been complete within the 75-ms pulse. However, we will continue to refer to currents at the end of the pulse as "steady-state" currents, for simplicity. Hence currents at each potential were averaged over two time periods: either the first

10 ms or the final 10 ms of each 75-ms episode (see Fig. 7). Apparent reversal potentials (V_{rev}) were identified by linear regression in the resulting current-voltage relations. These data were used to calculate relative permeabilities (P_X/P_{Cl}) according to the Goldman-Hodgkin-Katz equation in the following form:

$$\frac{P_X}{P_{Cl}} = \frac{[Cl^-]_r 10^{ZF\Delta V_r/RT} - [Cl^-]_t}{[X^-]_t}$$

where $[Cl^-]_r$ and $[Cl^-]_t$ are the concentrations of Cl^- in the reference and test solutions, respectively; $[X^-]_t$ is the concentration of anion X in the test solution (96 mM); ΔV_r is the change in reversal potential; and Z, R, T, and F have their usual meanings (Cohen et al., 1992). This method of calculation assumes that $[Cl]_{in}$ does not change drastically during the experiment, which is likely to be a safe assumption, because we kept the exposure to substitute anions brief. Reversal potentials were corrected for the presence of junction potentials (see Materials and Methods). Relative chord conductances (G_X/G_{Cl}) for anion entry at each time period were calculated from the change in current over a voltage range from approximately V_{rev} to a potential at least 25 mV depolarized from V_{rev}. By analyzing only the outward currents, we isolate the data for currents carried by mixtures of Cl and substitute anions under known conditions. Test anions were chosen to span a range of ionic radii, including small halides and several polyatomic anions up to 5.8 Å in diameter (gluconate).

Relative permeabilities for WT channels are given in Table 1. For most anions, the relative permeabilities are determined by their relative hydration energies, as expected for a channel with a lyotropic selectivity sequence (Tabcharani et al., 1997; McCarty and Zhang, 1998b). Two anions, iodide and perchlorate, exhibit relative permeabilities lower than expected from this relationship. Block of CFTR WT channels by iodide has been described by several investigators (Linsdell et al., 1997a; McCarty and Zhang, 1998b; Mansoura et al., 1998). This was initially attributed to interaction of this anion with R347 at the cytoplasmic end of TM6 in CFTR, based upon the loss of iodide block in R347D-CFTR. However, it has recently been shown that this mutation destroys a salt bridge that may be important in maintaining the conformation of the cytoplasmic vestibule (Cotten and Welsh, 1999). Interestingly, the relative permeability to perchlorate is drastically lower than expected for a weak-field site (Wright and Diamond, 1977), suggesting that the pore of CFTR can be described as a mixture of sites of varying field strengths. The relative permeabilities of isethionate, glutamate, and gluconate are very low (Table 1), as if these ions are too large to enter the pore.

Relative conductances are also determined by anion size (Table 1). In the WT, no anion exhibited conductance for anion entry greater than that of chloride (i.e., $G_X/G_{Cl} < 1$ for all substitute anions). In no case did we measure a zero conductance; WT channels exhibit a baseline conductance in the presence of substitute anions because all substitution solutions contain 4 mM residual chloride (see Materials and Methods). This allows us to separate the substitute anions into three classes with respect to conductance for anion entry (see Fig. 8, *B* and *D*): 1) anions that exhibit significant conductance, albeit less than that of chloride (nitrate and bromide); 2) anions that are too large to fit easily in the pore (glutamate, acetate, gluconate, and isethionate); and 3) anions that are small enough to fit in, but bind so tightly that they block current generated by the residual chloride (iodide, thiocyanate, and perchlorate). Much of the conductance in the presence of the large anions is due to the residual chloride in these anion substitution solutions, although there may be a low intrinsic conductance of the large anions themselves. It is also possible that the binding of sticky anions, such as perchlorate, in the vestibule of the channel, rather than in the pore proper, reduces the flux of the residual chloride by establishing a local negative surface charge (Dani et al., 1983).

TABLE 1 Selectivity in the WT channel at steady state

Ion	E_{rev} (mV)	P_X/P_{CI}	G_X/G_{CI}	Radius (Å)	$\Delta_{hydr}G°$ (kJ mol^{-1})
SCN	−54.54 ± 0.68	2.44 ± 0.07	0.21 ± 0.02	2.13	−287
NO_3	−38.28 ± 0.91	1.30 ± 0.02	0.93 ± 0.02	1.89	−306
Br	−32.68 ± 0.82	1.08 ± 0.01	0.76 ± 0.02	1.96	−321
Cl	−30.31 ± 0.64	1.0	1.0	1.81	−347
I	−9.71 ± 0.94	0.41 ± 0.01	0.29 ± 0.01	2.20	−283
Acetate	2.14 ± 1.28	0.26 ± 0.01	0.60 ± 0.02	2.32	−373
Glutamate	7.11 ± 1.44	0.22 ± 0.02	0.61 ± 0.03	2.75	—
Isethionate	8.69 ± 1.02	0.18 ± 0.01	0.48 ± 0.01	2.60	—
ClO_4	9.32 ± 0.71	0.17 ± 0.01	0.17 ± 0.01	2.40	−214
Gluconate	14.46 ± 1.68	0.16 ± 0.02	0.58 ± 0.01	2.90	—

Ions are listed in order of decreasing relative permeability.
Values listed for ionic radii are the effective radii reported by Marcus (1997), except those for glutamate (Franciolini and Nonner, 1987) and gluconate (Halm and Frizzell, 1992).
Values for the change in Gibbs free energy upon hydration ($\Delta_{hydr}G°$) are also from Marcus (1997).
Experimentally determined values are shown as the mean ± SE for $n = 5$ oocytes.

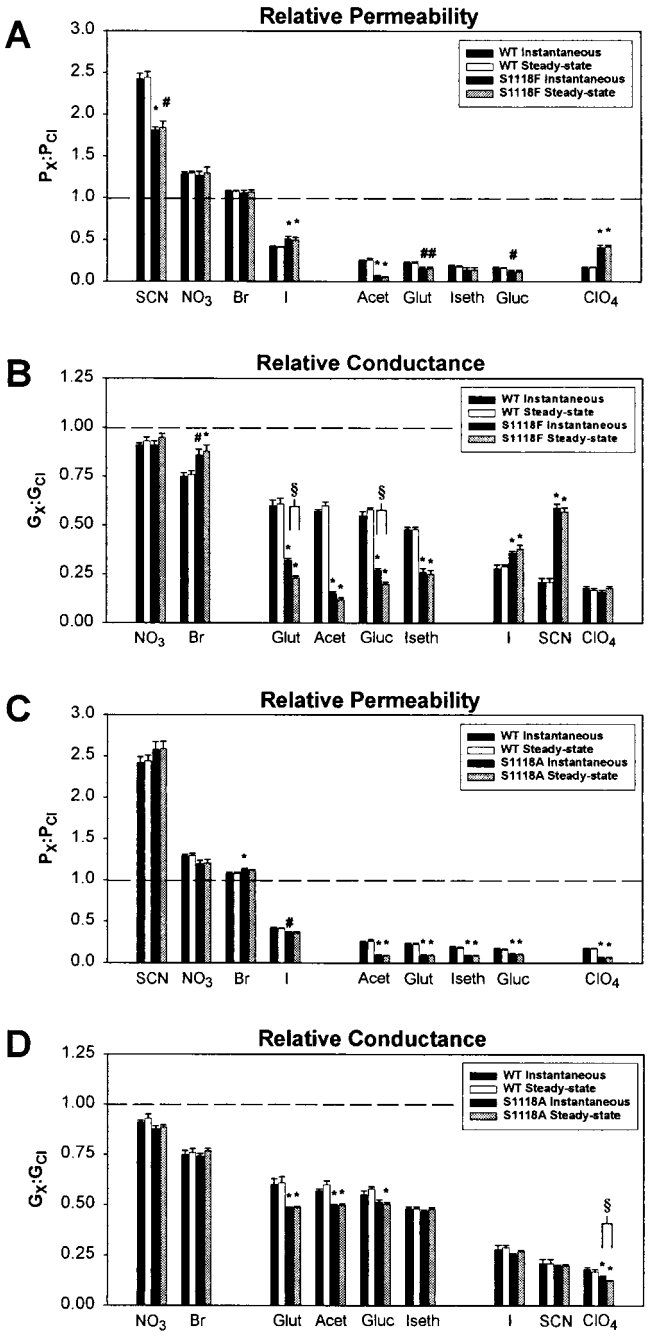

FIGURE 8 Selectivity data for WT CFTR as compared to S1118F-CFTR (*A* and *B*) and S1118A-CFTR (*C* and *D*). Relative permeabilities and relative conductances are listed in decreasing order for WT. The dashed line in all figures indicates equality to Cl. Mean ± SE. $^{*}p \leq 0.01$; $^{\#}p \leq 0.05$, compared to WT, for $n = 5$ for each combination. In each figure, data are separated according to the time during the voltage jump (refer to Fig. 7) so that selectivities early in the relaxation (from instantaneous currents) can be compared to selectivities late in the relaxation (from steady-state currents). Relative permeabilities and relative conductances were compared for WT or mutants, using data in each time segment. Differences between instantaneous and steady-state results are indicated by brackets. $^{\S}p < 0.01$ for S1118F-CFTR or $p = 0.02$ for S1118A-CFTR. WT data in *A* and *B* are repeated in *C* and *D* for ease of comparison.

In Fig. 8 anions are listed in order of decreasing relative permeability (Fig. 8, *A* and *C*) or decreasing relative conductance (Fig. 8, *B* and *D*) in the WT channel. Data are shown for both instantaneous currents and steady-state currents for WT and S1118F-CFTR (Fig. 8, *A* and *B*) or S1118A-CFTR (Fig. 8, *C* and *D*). In Cl^--containing solutions, before anion substitutions were made, there was a significant difference ($p = 0.047$) between instantaneous and steady-state reversal potentials in S1118F-CFTR (Table 2) compared to the WT (Table 1), but not in S1118A-CFTR. This suggests that S1118F-CFTR channels may be less Cl^--selective than are WT channels. Comparing the selectivity pattern in S1118F-CFTR with that of WT, without respect to time dependence, showed significant changes for both relative permeabilities and relative conductances (compare Tables 1 and 2). The ability of the large anions (acetate, gluconate, glutamate, and isethionate) to gain access to the pore is altered by mutations S1118A and S1118F, as indicated by mild to significant changes in relative permeabilities for these anions compared to that in WT channels. Interestingly, introduction of the hydrophobic Phe at S1118 reduced P_{SCN}/P_{Cl} and increased P_{ClO4}/P_{Cl} substantially. However, it is important to note that relative permeabilities (and/or relative conductances) for some substitute anions were not altered, suggesting that the mutations did not disrupt the global pore structure. S1118A-CFTR exhibited reduced relative permeabilities for all of the large anions and for perchlorate. However, neither the Phe nor the Ala substitutions changed the relative permeability sequence enough to eliminate the overall lyotropic character of the selectivity sequence. Furthermore, while relative permeabilities to iodide and perchlorate were increased with respect to WT, these values remained well below their expected values, based upon hydration energies.

As we and others have found (McCarty and Zhang, 1998b; Mansoura et al., 1998), relative conductances were more sensitive to mutation in pore-lining domains than were relative permeabilities. Accordingly, G_X/G_{Cl} in S1118F-CFTR showed dramatic changes for seven of the nine test anions (Fig. 8 *B*). Relative conductances for the large anions were altered substantially in the S1118F-CFTR. Whether this is due to a reduction in the absolute conductance for the large anions or a decrease in conductance by the residual 4 mM Cl^- is not known; however, patch-clamp experiments show that the single-channel conductance for Cl^- entry is reduced in the mutant in the presence of symmetrical high [Cl^-] (Fig. 5), consistent with the latter of these two possibilities. S1118F-CFTR also exhibited less block by iodide and thiocyanate, consistent with disruption of the high-affinity binding of these anions in the WT pore. Relative conductances were generally less affected in S1118A-CFTR than in S1118F-CFTR. In contrast, mutation S1118A had the greatest effects on P_X/P_{Cl} relationships, particularly for the large polyatomic anions (Fig. 8, *C* and *D*).

TABLE 2 Selectivity in S1118F-CFTR and S1118A-CFTR

	S1118F			S1118A		
Ion	E_{rev} (mV)	P_X/P_{Cl}	G_X/G_{Cl}	E_{rev} (mV)	P_X/P_{Cl}	G_X/G_{Cl}
SCN	−40.97 ± 1.20*	1.84 ± 0.08*	0.57 ± 0.02*	−56.44 ± 0.93	2.59 ± 0.09	0.20 ± 0.01
NO_3	−32.83 ± 1.69	1.30 ± 0.06	0.95 ± 0.02	−37.35 ± 0.87	1.21 ± 0.04	0.88 ± 0.01
Br	−28.28 ± 1.32	1.07 ± 0.03	0.88 ± 0.03*	−34.53 ± 0.85	1.12 ± 0.02	0.77 ± 0.01
Cl	−26.14 ± 1.59*	1.0	1.0	−30.63 ± 0.64	1.0	1.0
I	−8.46 ± 1.14	0.52 ± 0.03*	0.38 ± 0.03*	−10.35 ± 1.26	0.39 ± 0.01	0.27 ± 0.05
Acetate	39.64 ± 1.77*	0.05 ± 0.01*	0.12 ± 0.01*	23.24 ± 1.83*	0.09 ± 0.01*	0.50 ± 0.01*
Glutamate	23.93 ± 3.61*	0.16 ± 0.01*	0.23 ± 0.01* 0.32 ± 0.01[I]*	19.59 ± 1.07*	0.09 ± 0.01*	0.49 ± 0.01*
Isethionate	20.24 ± 3.62*	0.14 ± 0.03	0.25 ± 0.02*	23.71 ± 0.99*	0.09 ± 0.01*	0.48 ± 0.01
ClO_4	−6.42 ± 1.57*	0.42 ± 0.02*	0.18 ± 0.01	27.29 ± 1.36*	0.06 ± 0.01*	0.12 ± 0.01* 0.14 ± 0.01[I]*
Gluconate	28.26 ± 3.29*	0.12 ± 0.02	0.20 ± 0.01* 0.27 ± 0.01[I]*	20.03 ± 1.04*	0.10 ± 0.01*	0.50 ± 0.01*

Ions are listed in the same order as in Table 1. Data listed are for steady-state values (mean ± SE for $n = 5$ oocytes each), unless otherwise noted. Instantaneous values ([I]) are listed only when they differ from steady-state values.
*$p \leq 0.05$ compared to WT.

In comparing the instantaneous data (first 10 ms of the jump) with the steady-state data (last 10 ms), we found that there were no time-dependent changes in relative permeability or relative conductance for WT channels. Nor does relative permeability for S1118F-CFTR (Fig. 8 *A*) or S1118A-CFTR (Fig. 8 *C*) show any time dependence. However, relative conductances for the largest anions studied (gluconate and glutamate) decreased in S1118F-CFTR during the 75-ms voltage jump (Fig. 8 *B*;[§] indicates $p < 0.01$). Because these effects in S1118F-CFTR were only found for the largest anions tested, we propose that this result signifies a time-dependent change in the diameter of the narrowest part of the pore. We would expect this difference to be magnified in experiments in which Cl^- was replaced entirely with glutamate or gluconate (Khakh and Lester, 1999). However, such an experiment is not possible because of the low solubility of Mg^{2+}, which is required for the integrity of the oocyte membrane. As shown in Fig. 8 *D*, there was also a statistically significant time dependence of relative conductance to perchlorate for S1118A-CFTR ($p = 0.02$). We do not know the basis for this change.

Fig. 9 shows the current-voltage relations in the presence of chloride and glutamate for one representative experiment in S1118F-CFTR. For simplicity of comparison, the data have been shifted along the voltage axis so that the reversal potentials were equalized to zero. The reversal potentials for Cl^- and glutamate differ widely (Table 2) but were not time dependent. In contrast, the conductance in Cl^- over this narrow voltage range (the range used to calculate G_X/G_{Cl}) decreases, as a result of the voltage-jump relaxation. However, the conductance in glutamate decreased more than expected during the relaxation, resulting in a decrease in G_{Glut}/G_{Cl} for this experiment from 0.35 to 0.19.

Based upon the following observations, we reasoned that there may be a structural connection between the changes in permeation properties of S1118F-CFTR and the process underlying the voltage jump relaxations: 1) The change in permeation properties after a voltage jump (Figs. 1 and 9) is consistent with the steady-state kinetics of single channels (Fig. 5). 2) Inspection of the raw traces in Figs. 1 *C*, 2 *A*, and 2 *B* suggest that the direction of the relaxation reverses around the reversal potential of the macroscopic currents. 3) The steady-state *I*/*V* relation diverges from the instantaneous *I*/*V* relation with an inflection point at the potential at which the macroscopic currents reverse. This is seen most clearly after a depolarizing prepulse (Fig. 3 *A*). To address this issue, we asked whether there is any interaction between permeation and gating in S1118F-CFTR channels studied under whole-cell conditions. Oocytes expressing

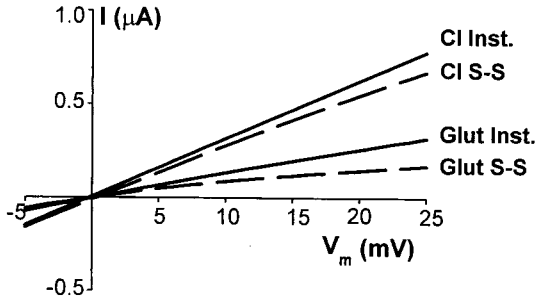

FIGURE 9 Decrease in relative conductance to glutamate at steady state. Current-voltage relations in chloride and glutamate for instantaneous currents (——) and steady-state currents (– – –) in S1118F-CFTR were adjusted on the voltage axis so that their reversal potentials were set to zero. Actual V_{rev} values were −13.90 and −13.23 mV for chloride and 14.99 and 15.37 mV (instantaneous and steady state, respectively) for glutamate, for the experiment shown. The slope conductances for both ions decrease during the relaxation. However, the relative conductance, G_{Glut}/G_{Cl}, calculated as the ratio of conductances from solid lines and conductances from dashed lines, changed from 0.35 to 0.19 during the relaxation.

WT or S1118F-CFTR channels were studied using the same voltage-clamp protocol as the one used for the data shown in Fig. 7. Current traces for the three most depolarizing potentials are shown in Fig. 10. When the predominant bath anion was Cl^-, WT channels did not show a relaxation after the initial clamp transient (Fig. 10 *A*), which was prolonged because of the use of an agar bridge to ground the preparation. Fitting the trace at +80 mV gave a time constant of several hours, as expected, because WT channels are time independent. When the predominant anion was SCN^-, however, WT currents showed a moderate degree of time dependence (τ = 70.3 ms at +80 mV). This may reflect the fact that even low concentrations of SCN^- inhibit Cl^- permeation in CFTR, leading to a decrease in whole-cell conductance (Table 1). As SCN^- enters the pore at depolarizing potentials, Cl^- conductance becomes blocked, leading to the appearance of a moderate relaxation.

S1118F-CFTR currents showed a relaxation as expected from previous experiments (Figs. 1, 2, and 7). In Cl^--containing bath, the time constant was in the range seen for experiments of the sort shown in Fig. 2 ($\tau \approx 22$ ms). However, when the bath contained SCN^- as the predominant anion, the relaxations were slowed by ~80% (Fig. 10 *B*). Because SCN^- blocks mutant channels as it does WT channels (Table 2), we would expect the time constant for S1118F-CFTR channels in the presence of SCN^- to be reduced as it is for WT channels. In contrast, the relaxations in S1118F-CFTR were slowed by this less permeant anion such that the process underlying the relaxations was not complete even by the end of the 75-ms voltage jump. Fig. 10 *C* shows that the time constant of the relaxation was lengthened in proportion to the reduced relative conductance shown for each test anion (compare to Fig. 8 *B*). Bromide is nearly as conductive as Cl^- in these channels (i.e., $G_{Br}/G_{Cl} \cong 1$). Hence it had only a small effect on the shift of the time constant of the relaxations (Fig. 10 *C*). However, the less conductive SCN^- ($G_{SCN}/G_{Cl} \ll 1$) had a much larger effect on the shift of the time constant of the relaxation. In summary, the lengthening of the gating process at positive potentials in S1118F-CFTR follows the relative conductance sequence. Anions that are less conductive in this channel have a greater effect on the time constant of the relaxation. This implies a distinct connection between permeation and gating in S1118F-CFTR.

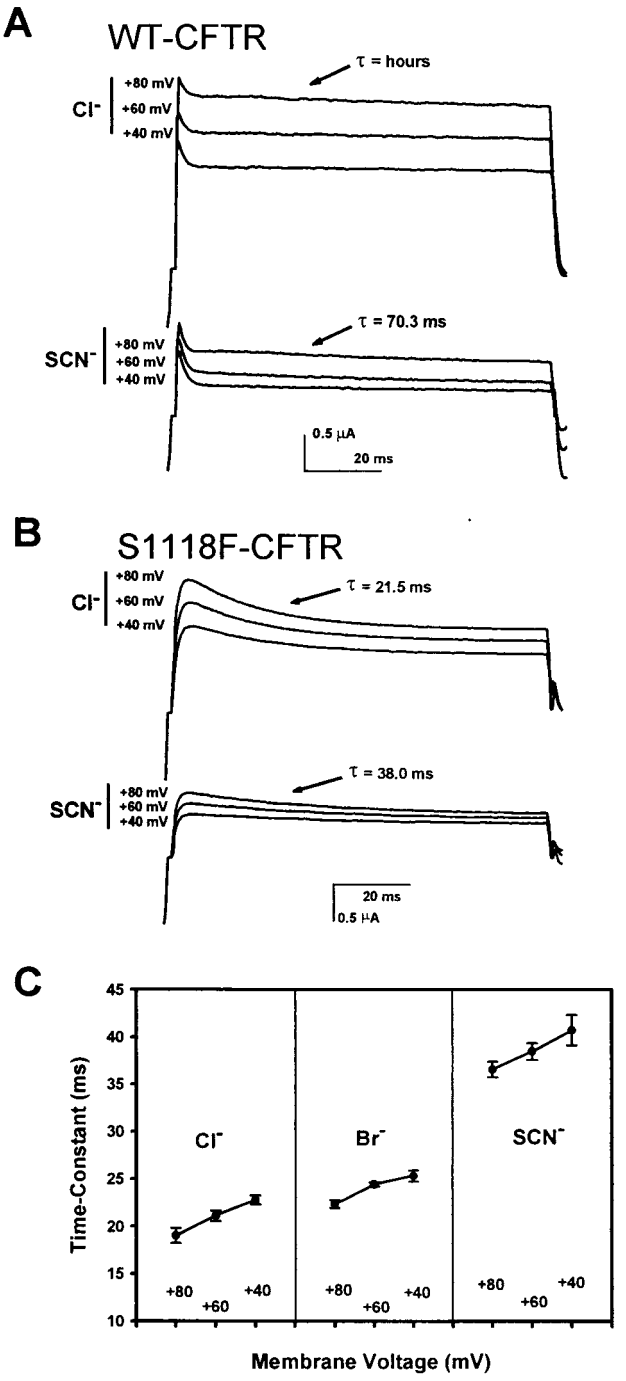

FIGURE 10 Interaction between permeation and gating. (*A*) Voltage-clamp currents at +80, +60, and +40 mV for WT in the presence of Cl^- (*top*) or SCN^- (*bottom*) as the predominant bath anion. (*B*) Mutant channels recorded in the same manner. (*C*) Time constants for the relaxations in WT and S1118F-CFTR channels were calculated by fitting the decay to an exponential function. Shown are the time constants (τ) for S1118F-CFTR currents recorded in bath solution containing Cl^-, Br^-, or SCN^-.

DISCUSSION

The primary structure of CFTR gave few clues to the portions of the protein that contribute to formation of the walls of the pore. In this study we have investigated the role of one residue in the 11th transmembrane helix. Mutation of this residue, S1118, has effects on both permeation and gating, which implies that TM11 may contribute to the pore. Substitutions by phenylalanine or cysteine at this position are associated with cystic fibrosis (Tsui, 2000). Our mea-

surements in S1118F-CFTR show modest current relaxations, on the order of 30%, during voltage jumps between −140 and +80 mV. These are the first reports of voltage-dependent gating by a CFTR variant.

Using a variety of approaches, structure/function studies in CFTR have led to the proposal of pore-lining roles for TM domains 1, 2, 3, 5, 6, and 12 (Anderson et al., 1991b; McDonough et al., 1994; Oblatt-Montal et al., 1994; Akabas et al., 1994; Cheung and Akabas, 1996, 1997; Akabas, 1998; Mansoura et al., 1998). The majority of work investigating point residues in the putative pore of CFTR has emphasized residues in or flanking TM6. Here it is believed that K335 and R347 influence selectivity and Cl^- conductance (Anderson et al., 1991b; Tabcharani et al., 1993; Mansoura et al., 1998), cysteine substitutions for several residues interact with sulfhydryl-specific reagents as if they face the pore (Cheung and Akabas, 1996), and the anion/cation selectivity filter is formed by three residues at the cytoplasmic end of TM6 (Cheung and Akabas, 1997; Guinamard and Akabas, 1999). Anomalous mole fraction effects (Tabcharani et al., 1993) and protocol-dependent block by iodide (Tabcharani et al., 1997) are lost in R347D-CFTR; this may be due to a severe disruption in secondary structure by the loss of a salt bridge between R347 and D924 (Cotten and Welsh, 1999). Selectivity in CFTR follows a lyotropic sequence, predominantly determined by the character of residues in TM6 (Tabcharani et al., 1997; Linsdell et al., 1997a,b). TM6 also governs channel rectification and affinity for the pore blockers DPC, NPPB (5-nitro-2-(3-phenylpropylamino)-benzoate), and glibenclamide (McDonough et al., 1994; Zhang and McCarty, 1998; Zhang et al., 2000). Residues in TM12 also contact these drugs (McDonough et al., 1994). Our preliminary evidence suggests that residues in TM12 also contribute to selectivity in CFTR (McCarty and Zhang, 1998b; Zhang et al., 2000), but no other TM domains in the C-terminal half of the CFTR molecule have been studied. The CFTR pore is apparently lined with several domains that have no strong influence on permeation. For example, although residues in TM1 are available to cysteine-specific reagents (Akabas et al., 1994), deletion of all of TM1 has no apparent effect on channel function (Carroll et al., 1995). Evidence to date points to TM6 as the major determinant of permeation. Similarly, some residues in TM5 and TM12 contact the pore; other transmembrane domains may stabilize channel opening, without contributing extensively to the energy profile of the channel. The present study shows that mutations at one position in TM11 alter anion selectivity, single-channel conductance, macroscopic rectification, and voltage-dependent blockade by DPC. These observations are consistent with a pore-lining role for TM11 in the functional CFTR channel.

S1118 lies at a position predicted to be between two important domains in the cross-sectional view of the pore (Fig. 1 *A*). On the basis of site-directed mutations in TM6 and TM12, we have described two cross-sectional levels in the pore wherein mutations have prominent effects on permeation properties and block by DPC. In particular, mutation T1134F in TM12 lowered single-channel conductance to ~6 pS and increased DPC affinity without changing the voltage dependence of block (McDonough et al., 1994). Mutation S341A in TM6 reduced affinity for DPC fivefold, induced inward rectification, and decreased the single-channel conductance to ~1 pS (McDonough et al., 1994). These residues are separated by two turns of the helices (Fig. 1 *A*). In TM6, between those two cross-sectional domains, at a position also predicted to face the pore, is T338. Mutation T338A altered the voltage dependence of block by DPC without affecting affinity at −100 mV (McDonough et al., 1994). Cysteine-scanning mutagenesis experiments did not identify T338 as a pore-lining residue (Cheung and Akabas, 1996; Cheung and Akabas, 1997). However, this may be due to steric hindrance limiting access of the sulfhydryl-modifying reagents to this region of the pore. We (McCarty and Zhang, 1999) and others (Linsdell et al., 1997b, 1998) have found that anion selectivity is highly sensitive to mutation at T338, suggesting that it may contribute to a region of high discrimination within the pore. Hence residues in this cross-sectional domain also appear to contribute to the multiple permeation properties of the pore. In our alignment, S1118 in TM11 is in a position homologous to that of T338 in TM6.

With respect to block by DPC, S1118F-CFTR had an effect much like that of T338A-CFTR, wherein affinity at −100 mV was not changed significantly but the voltage dependence was reduced. The absolute difference in the apparent K_D (at −100 mV) for DPC between wild type and S1118F-CFTR, taken by itself, is too small to conclude that residue S1118 lines the channel pore. Similarly, S1118A did not affect block by DPC (McDonough et al., 1994). However, both S1118A-CFTR and S1118F-CFTR altered the selectivity behavior of the pore, suggesting that this position may contribute to the pore walls. Relative conductances for many of the substitute anions were altered in S1118F-CFTR. In contrast, mutation S1118A exhibited the greatest effects on relative permeabilities, especially for the large anions. Relative permeability is independent of channel gating, because it is derived from zero-current measurements. However, relative conductances may not be independent of gating, as they are highly sensitive to anion binding (Dawson, 1996). If channel gating causes a conformational change in the pore such that the electrostatic field in which anions bind is altered, then gating may be expected to change the relative conductances to some or all anions. Indeed, we see this effect when the relative conductance to glutamate and to gluconate decreases during the voltage-jump relaxation. Furthermore, S1118F-CFTR also exhibits a reduced single-channel conductance. Taken together, these observations are consistent with a pore-facing position for S1118. However, the selectivity changes are most prom-

inent only for the largest anions tested and are mild compared to mutations at some positions in TM6 (McCarty and Zhang, 1998b, 1999). Therefore, it may be that TM11, at least at the cross-sectional level of S1118, contributes less to the walls of the pore than do TM6 and TM12.

Alterations in selectivity during gating of other channels have also been described (Khakh and Lester, 1999). For example, *Shaker* potassium channels mutated at T442 in the signature sequence visit subconductances en route to the full conductance state. In T442S channels, the subconductances and the full conductance have opposite selectivities between K^+, NH_4^+, and Rb^+, as well as alterations in rates of opening, suggesting that some of the same structures may be involved in channel gating and ion permeation (Zheng and Sigworth, 1997). P2X transmitter-gated cation channels exhibit permeability changes over a time course of seconds, in an activity-dependent manner (Khakh et al., 1999). These changes in selectivity were sensitive to mutation in the C-terminal TM domain.

In all systems reported thus far, wild-type single CFTR channels open for prolonged bursts lasting up to a few seconds (Foskett, 1998; Gadsby and Nairn, 1999). Channel opening is dependent upon the presence and hydrolysis of ATP (Anderson et al., 1991a; Baukrowitz et al., 1994; Zeltwanger et al., 1999). The single-channel conductance is linear in symmetrical 150 mM Cl^- and averages 8 pS in our hands at room temperature. S1118F-CFTR single channels differ doubly from wild-type channels. First, S1118F-CFTR openings are much briefer than wild-type openings (burst duration is reduced by 93%). The choppy bursts of S1118F-CFTR closely resemble the bursts of mutant R117H, a mutation that causes mild cystic fibrosis (Sheppard et al., 1993). Second, the single-channel conductance of S1118F-CFTR rectifies inwardly, in agreement with the steady-state rectification of macroscopic currents. The rectification of single-channel steady-state conductance for S1118F-CFTR arises primarily from decreased conductance at positive potentials, because the single-channel conductances for the WT and mutant are nearly equal at -100 mV but differ at $+100$ mV. Altered single-channel kinetics and conductance are also suggestive of the mutation of a pore-lining residue. That S1118F-CFTR has more defective conduction properties for positive current at depolarizing potentials (i.e., for inward flux of Cl^-) suggests that the mutated residue affects the channel at a point nearer the extracellular than the cytoplasmic end of the channel. In the model presented in Fig. 1, S1118 does lie toward the extracellular end of TM11.

Nonetheless, the usual concerns regarding the interpretation of data from site-directed mutagenesis must be remembered. There is a distinct possibility that the substitution of phenylalanine at this position perturbs another transmembrane domain, resulting in an indirect alteration of channel function. The shortened openings in S1118F-CFTR may reflect a destabilization of the global protein structure rather than a specific effect on the pore. Arguments against a destabilization of global structure include 1) preservation of some aspects of the permeability sequence; 2) retention of ATP dependence of single-channel openings, suggesting that any structural changes are at least not widespread enough to alter the interaction between the nucleotide binding domains and the membrane-spanning domains; 3) preservation of WT affinity for block by DPC at -100 mV; and 4) the observation that selectivity patterns were altered significantly by both alanine substitution and phenylalanine substitution, representing opposite ends of the spectrum in terms of subtlety of change in the side chain. Similarly, the current relaxations are not due to disruption of a putative interaction between S1118 and another amino acid, because no relaxations were observed for S1118A-CFTR. However, it is clear that further positions in TM11 must be studied in detail to solidify a pore-lining role for this transmembrane domain.

Macroscopic voltage-jump relaxations are usually explained on the basis of voltage-dependent changes in the fraction of time spent by a channel in the conducting state or states. The shift in the macroscopic I/V relation between instantaneous and steady-state measurements describes a sequence of states of the channel (Dawson, 1996). These changes can occur either because of 1) voltage-dependent channel opening and closing rates or 2) voltage-dependent block. Our results suggest that the mutant acquired an additional open-to-closed transition, with a time constant on the order of tens of milliseconds. The single-channel recordings confirm that S1118F-CFTR openings are interrupted to a much greater extent than wild-type openings. Furthermore, the openings and interruptions occur on a time scale of tens of milliseconds. Thus the single-channel data provide a qualitative explanation for the fact that macroscopic currents decrease on a time scale of tens of milliseconds during a jump to positive potentials and increase during a jump to negative potentials. Whether the interruptions are 1) gating transitions of the mutant channel protein or 2) block produced by the binding of an additional molecule is unclear. However, our experiments uncovered no evidence for block by Mg^{2+} or Ca^{2+} ions; blocking by known CFTR pore blockers occurs on a time scale roughly 10- to 100-fold faster than that of the relaxations (McCarty et al., 1993; McDonough et al., 1994; Zhang et al., 2000). Block by the pH buffers is unlikely, because different buffers were used for whole-cell and single-channel experiments. Thus there is no reason to suspect that the relaxations are produced by voltage-dependent blocking events, and we tentatively favor the explanation that the S1118F-CFTR has altered gating kinetics. Further experiments will be required to identify changes in single-channel kinetics and/or conductance in the brief time domain immediately after a voltage step, which would be indicative of discrete states. Although an additional state may have been added to the kinetic scheme for S1118F-CFTR, it is also possible that an existing state has been modified. For instance, it will be important to

determine if the prominent voltage-dependent fast flicker in WT observed at hyperpolarizing potentials is modified by the S1118F mutation.

Possible mechanisms

S1118F-CFTR exhibits alterations in permeation properties, as might be expected given the location of this mutation, but also exhibits alterations in single-channel gating. Gating of WT-CFTR occurs through interactions of the large cytoplasmic domains and involves phosphorylation of the protein, predominantly at the R-domain, and binding and hydrolysis of ATP at the NBDs (Gadsby and Nairn, 1997). Both of these processes occur on the time scale of seconds for the WT channel (Nagel et al., 1992). Although the possibility cannot be formally excluded, it seems unlikely that one or both of these processes are accelerated by factors of 10–100 to cause the voltage-dependent changes in open probability and rapid flickers seen in this mutant. It seems more likely that a unique process occurs for S1118F-CFTR. The most economical explanation for these time-dependent properties is that the mutated channel acquires a set of voltage-dependent closing events on the time scale of tens of milliseconds or faster. What is the physical basis of these events? Possibly the side chain of the newly introduced Phe is moving in and out of the channel, blocking it transiently. At the other end of the scale, the S1118F mutation might disrupt the stability of the protein global structure, leading to the observed effects on conduction. However, the preservation of several aspects of permeation and regulation argues against this notion.

Evidence for the movement of the Phe side chain within the pore comes from the observation that the changes in gating and permeation properties of the mutant display interaction. The rate of the relaxation depends upon the nature of the permeating anion, reminiscent of the gating of ClC-0 voltage-dependent chloride channels by the permeating anion (Pusch et al., 1995; Pusch, 1996). The relative conductance of the S1118F-CFTR channel to large anions decreases during the course of the relaxations, which may indicate that either the large anions are more capable of blocking the channels in the steady-state conformation, or that Cl^- permeation becomes blocked by an intrinsic portion of the protein in the steady-state conformation. The observations that the steady-state macroscopic I/V relation shows rectification of outward currents (Fig. 6 *C*) and that the single-channel conductance of outward currents in the absence of large anions is reduced (Fig. 5) support the latter of these two possible explanations. Hence the decay in macroscopic conductance at +80 mV in the mutant may relate to the introduction of a barrier to permeation during the 75 ms of the voltage step. We propose that the Phe group of the mutant provides this barrier and that the side chain starts out in a position permissive to conduction of chloride but then, after a depolarizing voltage pulse, swings into the cylindrical volume of the pore during the relaxation and blocks current flow.

The aforementioned hypothesis requires that there be a conformational change within the pore during the voltage jump, which leads to the movement of the side chain. Gating in CFTR has been thought, until recently, to involve only the large cytoplasmic domains. In this view, the pore-lining domains form a static barrel. However, three recent studies suggest that there may also be an involvement of the transmembrane domains in gating or that, at the least, the conformation of the pore is not static. First, block of the channel by intracellular 3-(N-morpholino)propanesulfonic acid occurs at a rate that is dependent upon whether the channel is in a highly activated state or a poorly activated state (Ishihara and Welsh, 1997). Second, mutations in putative TM domains at positions that contribute to the selectivity pattern of CFTR alter the sensitivity to activating conditions (Mansoura et al., 1998, and our unpublished observations). Finally, the asymmetrical permeability of large anions in CFTR is dependent upon ATP hydrolysis; in essence, the selectivity of the channel differs from normal when the ATP hydrolysis cycle is disrupted (Linsdell and Hanrahan, 1998). Our measurements may provide concrete evidence that the TM domains do change conformation during gating. Because phenylalanine is not charged, it is unlikely that it provides a voltage sensor of the sort found in true voltage-gated channels. It may be that conformational changes in the transmembrane domains of CFTR do occur in the WT channel, but are not evident because they 1) occur too fast to be resolved or 2) require a reporter group to make them clear. The S1118F mutation may provide this reporter group in the form of the Phe side chain and/or slow the relaxations to a rate that is resolvable in macroscopic recordings.

The authors thank Drs. H.A. Lester and S. Zeltwanger for comments on the manuscript.

This research was sponsored in part by the National Institutes of Health (DK-47027 and National Research Service Award to SIM), the Cystic Fibrosis Foundation (MCCART96P0), and the American Heart Association (9820032SE).

REFERENCES

Akabas, M. H. 1998. Channel-lining residues in the M3 membrane-spanning segment of the cystic fibrosis transmembrane conductance regulator. *Biochemistry.* 37:12233–12240.

Akabas, M. H., C. Kaufmann, T. A. Cook, and P. Archdeacon. 1994. Amino acid residues lining the chloride channel of the cystic fibrosis transmembrane conductance regulator. *J. Biol. Chem.* 269: 14865–14868.

Anderson, M. P., H. A. Berger, D. P. Rich, R. J. Gregory, A. E. Smith, and M. J. Welsh. 1991a. Nucleoside triphosphates are required to open the CFTR chloride channel. *Cell.* 67:775–784.

Anderson, M. P., R. J. Gregory, S. Thompson, D. W. Souza, S. Paul, R. C. Mulligan, A. E. Smith, and M. J. Welsh. 1991b. Demonstration that

CFTR is a chloride channel by alteration of its anion selectivity. *Science.* 253:202–205.

Baukrowitz, T., T.-C. Hwang, A. C. Nairn, and D. C. Gadsby. 1994. Coupling of CFTR Cl^- channel gating to an ATP hydrolysis cycle. *Neuron.* 12:473–482.

Bear, C. E., F. Duguay, A. L. Naismith, N. Kartner, J. W. Hanrahan, and J. R. Riordan. 1991. Cl− channel activity in *Xenopus* oocytes expressing the cystic fibrosis gene. *J. Biol. Chem.* 266:19142–19145.

Bear, C. E., C. Li, N. Kartner, R. J. Bridges, T. J. Jensen, M. Ramjeesingh, and J. R. Riordan. 1992. Purification and functional reconstitution of the cystic fibrosis transmembrane conductance regulator (CFTR). *Cell.* 68: 809–818.

Carroll, T. P., M. M. Morales, S. B. Fulmer, S. S. Allen, T. R. Flotte, G. R. Cutting, and W. B. Guggino. 1995. Alternate translation initiation codons can create functional forms of cystic fibrosis transmembrane conductance regulator. *J. Biol. Chem.* 270:11941–11946.

Cheung, M., and M. H. Akabas. 1996. Identification of cystic fibrosis transmembrane conductance regulator channel-lining residues in and flanking the M6 membrane-spanning segment. *Biophys. J.* 70: 2688–2695.

Cheung, M., and M. H. Akabas. 1997. Locating the anion-selectivity filter of the cystic fibrosis transmembrane conductance regulator (CFTR) chloride channel. *J. Gen. Physiol.* 109:289–299.

Cohen, B. N., C. Labarca, N. Davidson, and H. A. Lester. 1992. Mutations in M2 alter the selectivity of the mouse nicotinic acetylcholine receptor for organic and alkali metal cations. *J. Gen. Physiol.* 100:373–400.

Cotten, J. F., and M. J. Welsh. 1999. Cystic fibrosis-associated mutations at arginine 357 alter the pore architecture for CFTR: Evidence for disruption of a salt bridge. *J. Biol. Chem.* 274:5429–5435.

Dani, J. A., J. A. Sanchez, and B. Hille. 1983. Lyotropic anions: Na channel gating and Ca electrode response. *J. Gen. Physiol.* 81:255–281.

Dawson, D. C. 1996. Permeability and conductance of ion channels: a primer. *In* Molecular Biology of Membrane Transport Disorders. S. G. Schultz, editor. Plenum Press, New York. 87–110.

Devidas, S., H. Yue, and W. B. Guggino. 1998. The second half of the cystic fibrosis transmembrane conductance regulator forms a functional chloride channel. *J. Biol. Chem.* 273:29373–29380.

Drumm, M. L., H. A. Pope, W. H. Cliff, J. M. Rommens, S. A. Marvin, L.-C. Tsui, F. S. Collins, R. A. Frizzell, and J. M. Wilson. 1990. Correction of the cystic fibrosis defect in vitro by retrovirus-mediated gene transfer. *Cell.* 62:1227–1233.

Fischer, H., and T. E. Machen. 1994. CFTR displays voltage dependence and two gating modes during stimulation. *J. Gen. Physiol.* 104:541–566.

Foskett, J. K. 1998. ClC and CFTR chloride channel gating. *Annu. Rev. Physiol.* 60:689–717.

Franciolini, F., and W. Nonner. 1987. Anion and cation permeability of a chloride channel in rat hippocampal neurons. *J. Gen. Physiol.* 90: 453–478.

Gadsby, D. C., and A. C. Nairn. 1997. Regulation of CFTR channel gating. *Trends Biochem. Sci.* 19:512–518.

Gadsby, D. C., and A. C. Nairn. 1999. Control of CFTR channel gating by phosphorylation and nucleotide hydrolysis. *Physiol. Rev.* 70:S77–S107.

Guinamard, R., and M. H. Akabas. 1999. Arg^{352} is a major determinant of charge selectivity in the cystic fibrosis transmembrane conductance regulator chloride channel. *Biochemistry.* 38:5528–5537.

Halm, D. R., and R. A. Frizzell. 1992. Anion permeation in an apical membrane chloride channel of a secretory epithelial cell. *J. Gen. Physiol.* 99:339–366.

Higgins, C. F. 1992. ABC transporters: from microorganisms to man. *Annu. Rev. Cell Biol.* 8:67–113.

Ishihara, H., and M. J. Welsh. 1997. Block by MOPS reveals a conformational change in the CFTR pore produced by ATP hydrolysis. *Am. J. Physiol.* 273:C1278–C1289.

Kartner, N., J. W. Hanrahan, T. J. Jensen, A. L. Naismith, S. Sun, C. A. Ackerley, E. F. Reyes, L.-C. Tsui, J. M. Rommens, C. E. Bear, and J. R. Riordan. 1991. Expression of the cystic fibrosis gene in non-epithelial invertebrate cells produces a regulated anion conductance. *Cell.* 64: 681–691.

Khakh, B. S., X. R. Bao, C. Labarca, and H. A. Lester. 1999. Neuronal P2X transmitter-gated cation channels change their ion selectivity in seconds. *Nature Neurosci.* 2:322–330.

Khakh, B. S., and H. A. Lester. 1999. Dynamic selectivity filters in ion channels. *Neuron.* 23:653–658.

Linsdell, P., and J. W. Hanrahan. 1998. Adenosine triphosphate-dependent asymmetry of anion permeation in the cystic fibrosis transmembrane conductance regulator chloride channel. *J. Gen. Physiol.* 111:601–614.

Linsdell, P., J. A. Tabcharani, and J. W. Hanrahan. 1997a. Multi-ion mechanism for ion permeation and block in the cystic fibrosis transmembrane conductance regulator chloride channel. *J. Gen. Physiol.* 110:365–377.

Linsdell, P., J. A. Tabcharani, J. M. Rommens, Y.-X. Hou, X.-B. Chang, L.-C. Tsui, J. R. Riordan, and J. W. Hanrahan. 1997b. Permeability of wild-type and mutant cystic fibrosis transmembrane conductance regulator chloride channels to polyatomic anions. *J. Gen. Physiol.* 110: 355–364.

Linsdell, P., S.-X. Zheng, and J. W. Hanrahan. 1998. Non-pore lining amino acid side chains influence anion selectivity of the human CFTR Cl^- channel expressed in mammalian cell lines. *J. Physiol. (Lond.).* 512:1–16.

Mansoura, M. K., S. S. Smith, A. D. Choi, N. W. Richards, T. V. Strong, M. L. Drumm, F. S. Collins, and D. C. Dawson. 1998. Cystic fibrosis transmembrane conductance regulator (CFTR) anion binding as a probe of the pore. *Biophys. J.* 74:1320–1332.

Marcus, Y. 1997. Ion Properties. Marcel Dekker, New York.

McCarty, N. A., S. McDonough, B. N. Cohen, J. R. Riordan, N. Davidson, and H. A. Lester. 1993. Voltage-dependent block of the cystic fibrosis transmembrane conductance regulator Cl^- channel by two closely related arylaminobenzoates. *J. Gen. Physiol.* 102:1–23.

McCarty, N. A., and Z.-R. Zhang. 1998a. Interaction between permeation and gating studied in a pore-domain mutant in CFTR. *Biophys. J.* 74:396 (Abstr.).

McCarty, N. A., and Z.-R. Zhang. 1998b. Residues near the extracellular end of TM6 and TM12 in CFTR contribute to anion selectivity. *Biophys. J.* 74:A395 (Abstr.).

McCarty, N. A., and Z.-R. Zhang. 1999. Building a three-dimensional model of permeation in the CFTR Cl channel. *FASEB J.* 13:A70.

McDonough, S. I. 1994. Pharmacology and pore-forming domains of the cystic fibrosis transmembrane conductance regulator. Dissertation. Division of Biology, California Institute of Technology, Pasadena, CA.

McDonough, S., N. Davidson, H. A. Lester, and N. A. McCarty. 1994. Novel pore-lining residues in CFTR that govern permeation and open-channel block. *Neuron.* 13:623–634.

McDonough, S., Z.-R. Zhang, N. Davidson, H. A. Lester, and N. A. McCarty. 1998. Voltage-jump relaxations in a CFTR mutant. *Biophys. J.* 74:395 (Abstr.).

Nagel, G., T.-C. Hwang, K. L. Nastiuk, A. C. Nairn, and D. C. Gadsby. 1992. The protein kinase A-regulated cardiac Cl^- channel resembles the cystic fibrosis transmembrane conductance regulator. *Nature.* 360: 81–84.

Oblatt-Montal, M., G. L. Reddy, T. Iwamoto, J. M. Tomich, and M. Montal. 1994. Identification of an ion channel-forming motif in the primary structure of CFTR, the cystic fibrosis chloride channel. *Proc. Natl. Acad. Sci. USA.* 91:1495–1499.

Pusch, M. 1996. Knocking on channel's door: the permeating chloride ion acts as the gating charge in CIC-0. *J. Gen. Physiol.* 108:233–236.

Pusch, M., U. Ludewig, A. Rehfeldt, and T. J. Jentsch. 1995. Gating of the voltage-dependent chloride channel ClC-0 by the permeant anion. *Nature.* 373:527–531.

Rich, D. P., M. P. Anderson, R. J. Gregory, S. H. Cheng, S. Paul, D. M. Jefferson, J. D. McCann, K. W. Klinger, A. E. Smith, and M. J. Welsh. 1990. Expression of cystic fibrosis transmembrane conductance regulator corrects defective chloride channel regulation in cystic fibrosis airway epithelial cells. *Nature.* 347:358–363.

Riordan, J. R., J. M. Rommens, B.-S. Kerem, N. Alon, R. Rozmahel, Z. Grzelczak, J. Zielenski, S. Lok, N. Plavsic, J.-L. Chou, M. L. Drumm,

M. C. Iannuzzi, F. S. Collins, and L.-C. Tsui. 1989. Identification of the cystic fibrosis gene: cloning and characterization of complementary DNA. *Science.* 245:1066–1072.

Sheppard, D. N., D. P. Rich, L. S. Ostedgaard, R. J. Gregory, A. E. Smith, and M. J. Welsh. 1993. Mutations in CFTR associated with mild disease form Cl^- channels with altered pore properties. *Nature.* 362:160–164.

Sheppard, D. N., and M. J. Welsh. 1999. Structure and function of the CFTR chloride channel. *Physiol. Rev.* 79:S23–S45.

Tabcharani, J. A., P. Linsdell, and J. W. Hanrahan. 1997. Halide permeation in wild-type and mutant cystic fibrosis transmembrane conductance regulator chloride channels. *J. Gen. Physiol.* 110:341–351.

Tabcharani, J. A., J. M. Rommens, Y.-X. Hou, X.-B. Chang, L.-C. Tsui, J. R. Riordan, and J. W. Hanrahan. 1993. Multi-ion pore behavior in the CFTR chloride channel. *Nature.* 366:79–82.

Tsui, L.-C. 2000. CFTR Mutation Table. Cystic Fibrosis Consortium (http:www.genet.sickkids.on.ca/cftr-cgi-bin/FullTable).

Woodhull, A. M. 1973. Ionic blockage of sodium channels in nerve. *J. Gen. Physiol.* 61:687–708.

Wright, E. M., and J. M. Diamond. 1977. Anion selectivity in biological systems. *Physiol. Rev.* 57:109–156.

Zeltwanger, S., F. Wang, G.-T. Wang, K. D. Gillis, and T.-C. Hwang. 1999. Gating of cystic fibrosis transmembrane conductance regulator chloride channels by adenosine triphosphate hydrolysis: quantitative analysis of a cyclic gating scheme. *J. Gen. Physiol.* 113:541–554.

Zerhusen, B., J. Zhao, J. Xie, P. B. Davis, and J. Ma. 1998. A single conductance pore for chloride ions formed by two cystic fibrosis transmembrane conductance regulator molecules. *J. Biol. Chem.* 274: 7627–7630.

Zhang, Z.-R., and N. A. McCarty. 1998. A comparison of probes for structure/function experiments in CFTR. *Pediatr. Pulmonol. Suppl.* 17: 224–225.

Zhang, Z.-R., S. Zeltwanger, and N. A. McCarty. 2000. Direct comparison of NPPB and DPC as probes of CFTR expressed in *Xenopus* oocytes. *J. Membr. Biol.* 175:35–52.

Zheng, J., and F.J. Sigworth. 1997. Selectivity changes during activation of mutant *Shaker* potassium channels. *J. Gen. Physiol.* 110:101–117.